Nuclear Magnetic Resonance Studies of Hydrogen Diffusion in $LaNi_{5.0}H_{6.0}$ and $LaNi_{4.8}Sn_{0.2}H_{5.8}$

G. Majer, U. Kaess
Max-Planck-Institut für Metallforschung,
Heisenbergstr. 1, 70569 Stuttgart, Germany

and

R.C.Bowman, Jr.
Jet Propulsion Laboratory, California Institute of Technology,
4800 Oak Grove Dr., Pasadena, CA 91109-8099, USA

Abstract

Diffusion measurements of hydrogen in $LaNi_{5.0}H_{6.0}$ and $LaNi_{4.8}Sn_{0.2}H_{5.8}$ were carried out between 270 K and 365 K using the alternating pulsed field gradient nuclear magnetic resonance (APFG-NMR) technique. The diffusivity of hydrogen in $LaNi_{4.8}Sn_{0.2}H_{5.8}$ is characterized by a higher mobility and a lower activation enthalpy than observed in $LaNi_{5.0}H_{6.0}$. The diffusivities at room-temperature, $D(300\ \mathrm{K})$, are $9.2{\cdot}10^{-12}\mathrm{m^2s^{-1}}$ and $3.8{\cdot}10^{-12}\mathrm{m^2s^{-1}}$ for $LaNi_{4.8}Sn_{0.2}H_{5.8}$ and $LaNi_{5.0}H_{6.0}$, respectively. A fit of an Arrhenius expression, $D = D_0 \exp(-H_a/k_BT)$, to the diffusivities yields an activation enthalpy of $H_a = 0.29$ eV for $LaNi_{5.0}H_{6.0}$ and $H_a = 0.22$ eV for $LaNi_{4.8}Sn_{0.2}H_{5.8}$. The NMR spin-lattice relaxation rates Γ_1 and $\Gamma_{1\rho}$ were measured on the same samples in the temperature range between 100 K and 350 K. The D values and the relaxation data are shown to be consistent and are interpreted in terms of a diffusion mechanism involving at least two stages of hydrogen motion.

1. Introduction

The highly favorable hydrogen storage properties of $LaNi_5H_x$ and related systems have made them the subject of many investigations. In spite of intensive research, fundamental properties of these systems such as metal-hydrogen interaction and hydrogen diffusion behavior are still under discussion. NMR line-widths measurements of protons (deuterons) in $LaNi_5H_x$ ($LaNi_5D_x$) [1] and proton relaxation rate measurements [2, 3, 4, 5] have been conducted in an effort to understand the microscopic nature of hydrogen motion. The NMR wide-line spectra show both narrow and broad resonances within certain temperature ranges [1]. The proton spin-lattice relaxation rate, measured either in the laboratory frame, Γ_1, or in the rotating frame, $\Gamma_{1\rho}$, indicates that hydrogen motion proceeds via a complex mechanism, with multiple site occupancy and at least two types of thermally activated jump processes [5]. The dipolar contribution to the relaxation rate, $\Gamma_{1,\mathrm{d}}$ and $\Gamma_{1\rho,\mathrm{d}}$, is characterized by unequal slopes on the low and high-temperature sides of the $\ln(\Gamma_{1,\mathrm{d}})$ and $\ln(\Gamma_{1\rho,\mathrm{d}})$ versus T^{-1} curves. Furthermore, $\Gamma_{1\rho}$ studies performed at different resonance frequencies in the rotating frame, $\omega_1/2\pi$, indicate at low temperatures $\Gamma_{1\rho,\mathrm{d}} \sim \omega_1^{-1.35}$ [6], while $\Gamma_{1\rho,\mathrm{d}} \sim \omega_1^{-2}$ is expected for a single thermally activated process. In β-$LaNi_{5-y}Al_yH_x$, Al substitution for Ni increases H_a with subsequent reduction in the apparent diffusion coefficient by more than two orders of magnitude going from $y = 0$ to $y = 1.5$ [8]. A similar behavior was found for hydrogen diffusion in $LaNi_4BH_{1.5}$ [5]. Owing to the lack of lattice-specific theories for the complex hydrogen sublattices in these systems, all analyses of the proton spin-lattice relaxation rates are based on Lorentzian spectral density functions introduced by Bloembergen, Purcell and Pound [9] (BPP-functions).

As an alternative to relaxation rate measurements, the use of pulsed magnetic field gradients provides a direct access to the long-range diffusivity D [10]. In the case of powdered $LaNi_5H_x$, the random variation of the magnetization causes large nonuniform background magnetic field gradients G_i. Thus, for a correct measurement of the diffusivity alternating pulsed field gradients (APFG) are required in order to eliminate contributions from the cross term between the applied gradients and the random background gradients [11, 12]. Karlicek and Lowe measured the diffusivity of hydrogen in $LaNi_5H_{6.5}$ between 331 K and 375 K using the APFG-technique [12]. In the present work, we also applied the APFG-NMR to study hydrogen diffusion in $LaNi_{5.0}H_{6.0}$ with the goal to extend the range of the diffusion data to lower temperatures. A further aim of our work is to investigate the change in the diffusivity if in $LaNi_5H_x$ Ni is partly substituted by Sn. Tin substitution for nickel produces substantial decrease in the plateau pressure along with reductions in the absorption-desorption hysteresis ratios [13, 14]. Since the $LaNi_{5-x}Sn_x$ alloys have shown greatly enhanced stability of the hydride storage capacity during both thermal [15] and electrochemical [16] cycling, these

alloys are very promising candidates for several technological applications. Therefore, we measured the hydrogen diffusion in $LaNi_{4.8}Sn_{0.2}H_{5.8}$ by means of APFG-NMR for temperatures between 270 K and 350 K. The diffusion data are discussed together with information deduced from the proton spin-lattice relaxation rates Γ_1 and $\Gamma_{1\rho}$ that we measured at the same samples.

2. Experimental details

The preparation and characterization of the high-purity $LaNi_{5.0}H_{6.0}$ sample has been previously described by Spada et al. [5] when the sample was used for proton relaxation time measurements. The starting alloy $LaNi_{4.8}Sn_{0.2}$ had been prepared at the Iowa State University, Ames Laboratory. The $LaNi_{4.8}Sn_{0.2}H_{5.8}$ sample for the present NMR experiments had been prepared by reacting powder contained in a 7 mm o.d. quartz tube with hydrogen gas following the procedures of Spada et al. [5] except the maximum pressure was below 1.5 bar. The bottom of the tube with the hydrided powder was cooled in liquid nitrogen while the tube was sealed with a flame [15].

The proton relaxation rates Γ_1 were measured with the same Bruker NMR spectrometer previously used by Spada et al. [5]. The spin-lattice relaxation rates Γ_1 were determined at a resonance frequency of $\omega_0/2\pi = 34.5$ MHz via the inversion-recovery method. The measurements of the relaxation rates in the rotating-frame, $\Gamma_{1\rho}$, were performed employing a spin-locking field of 7.3 G, corresponding to $\omega_1/2\pi = 31.0$ kHz, at $\omega_0/2\pi = 34.5$ MHz for $LaNi_{5.0}H_{6.0}$ and $\omega_0/2\pi = 45.7$ MHz for $LaNi_{4.8}Sn_{0.2}H_{5.8}$.

The diffusivities were measured employing the alternating pulsed field gradient (APFG) technique proposed by Karlicek and Lowe [11]. The applied APFG-sequence consists of five 180^0 rf-pulses as illustrated in Fig. 1. Typical operating conditions were gradient pulse length $\delta = 0.5$ ms and time between two 180^0 rf-pulses $2\tau = 1.6$ ms. The gradient coils are of anti-Helmholtz type with an inductivity of about 1 mH and an inner diameter of 26 mm and are fixed in the 89 mm room-temperature bore of a superconducting magnet. The positive and negative gradients required in an APFG experiment are produced by separate home-built current supplies. Field gradient pulses up to 25 T m^{-1} corresponding to a current of 60 A through the gradient coils are obtained with high reproducibility and linearity over the sample volume of about 0.5 cm^3. A fine adjustment assures that the negative and positive gradient pulses have the same size.

The NMR-signals were observed at a resonance frequency of 37.7 MHz with a home-built Fourier-transform spectrometer using phase-alternating pulse schemes and quadrature detection. In order to improve the signal-to-noise ratio, signal averaging was per-

formed up to 200 times.

The sample temperature was monitored with two Pt-PtRh thermocouples placed slightly above and below the sample. The temperatures were stabilized by means of a digital PID controller combined with ohmic heating. Temperatures below room-temperature were achieved by cooling with cold nitrogen gas.

For the APFG-measurements the amplitude of the gradient pulses, G_A, was varied in 18 steps and the corresponding echo amplitude of the nuclear magnetization [11],

$$M(10\tau) = M_0(10\tau) \cdot \exp\Big[-\gamma^2 D\Big(\frac{10}{3} G_0^2 \tau^3 + 12 I_3^2 \tau + 4 I_2 - 4 I_3 I_1\Big)\Big] \qquad (1)$$

with

$$I_1 = \int_0^{\delta} \int_0^{t'} G(t'')dt''dt', \qquad I_2 = \int_0^{\delta} \Big[\int_0^{t'} G(t'')dt'' \Big]^2 dt', \qquad I_3 = \int_0^{\delta} G(t')dt', \qquad (2)$$

was measured at the time $t = 10\tau$. In Eq. (1) $\gamma = 2.6752 \cdot 10^8$ rad $s^{-1}T^{-1}$ denotes the gyromagnetic ratio of the proton and G_0 is a background field gradient. It is an important feature that in Eqs. (1) and 2), there is no cross term $G_A \cdot G_0$ contributing to the echo-attenuation, as it is the case for simpler PFG-sequences [10]. Thus, the APFG-technique permits the diffusivity to be measured independent of G_0, and herewith independent of the random background gradients G_i contributing to G_0. The deviations from the rectangular shape of the gradient pulses with nominal length δ and amplitude G_A are taken into account by measuring the time dependent current through the gradient coil at a calibrated resistor. Subsequently, this signal is digitized in a 10 MHz transient recorder with 12 bit resolution and the integrals in Eq. (2) are numerically evaluated. The diffusivity D follows from the slope of a plot of $\ln\Big(M(G_A, 10\tau)\Big)$ versus $\gamma^2\Big(\frac{10}{3} G_0^2 \tau^3 + 12 I_3^2 \tau + 4 I_2 - 4 I_3 I_1\Big)$.

3. Results and discussion

The diffusivities of hydrogen in $LaNi_{5.0}H_{6.0}$ and $LaNi_{4.8}Sn_{0.2}H_{5.8}$ measured by APFG-NMR are shown in Fig. 2. Within the investigated temperature range, the D values for each sample are well represented be a single Arrhenius law, $D = D_0 \exp(-H_a/k_B T)$, with the diffusion parameters given in table 1. The diffusivities measured at 300 K, $D(300\,\mathrm{K})$, are also included in this table. Karlicek and Lowe [12] performed APFG-measurements of hydrogen diffusion in $LaNi_5H_{6.5}$ between 331 K and 375 K. Their results, which are shown as a dashed line in Fig. 2, correspond to $D(300\,\mathrm{K}) = 1.4 \cdot 10^{-12}\,\mathrm{m^2 s^{-1}}$ and $H_a = 0.42$ eV. The larger H_a and slower D measured by Karlicek and Lowe for $LaNi_5H_{6.5}$ compared to the present results may be attributed to the larger hydrogen content in their sample. This type of change with increasing hydrogen content

has been noted previously in several metal hydrides [17, 18, 19, 20]. Richter et al. studied the hydrogen diffusivity in $LaNi_5H_6$ by quasi-elastic neutron scattering [21]. They found for the diffusivity at room-temperature $D(300\,K) = 5.0{\cdot}10^{-12}\ m^2s^{-1}$, in very good agreement with the present results. Züchner et al. [22] observed by electrochemical measurements in $LaNi_5H_x$ diffusion coefficients at room-temperature between $2.03{\cdot}10^{-12}\ m^2s^{-1}$ and $2.70{\cdot}10^{-12}\ m^2s^{-1}$ depending on the orientation of the $LaNi_5$ crystal. Recent magnetic after-effect measurements [23] yielded $H_a = 0.29$ eV in $La(Ni_{0.7}Fe_{0.3})_5H_2$ and $H_a = 0.32$ eV in $La(Ni_{0.7}Fe_{0.3})_5H_{0.7}$, which agree well with the activation enthalpies measured in $LaNi_5H_6$ by quasi-elastic neutron scattering [21], $H_a = 0.275$ eV, and by the APFG-studies of the present work, $H_a = 0.29$ eV.

An interesting feature of the present APFG-results is that the diffusivity D is higher and the activation enthalpy H_a is smaller in $LaNi_{4.8}Sn_{0.2}H_{5.8}$ compared to $LaNi_{5.0}H_{6.0}$. The Γ_1 and $\Gamma_{1\rho}$ data measured on the same samples also indicate a higher hydrogen mobility in $LaNi_{4.8}Sn_{0.2}H_{5.8}$. It is evident from Fig. 3 that in this system the Γ_1 and $\Gamma_{1\rho}$ maxima are both observed at lower temperatures than in $LaNi_{5.0}H_{6.0}$. By contrast, a reduction in the hydrogen mobility and an increase in the effective activation enthalpy is reported for the substitution of aluminum for nickel in $LaNi_5H_x$ [7, 8]. In metal-hydrides the proton relaxation rate may be decomposed according to

$$\Gamma_1 = \Gamma_{1,e} + \Gamma_{1,d}. \tag{3}$$

The electronic contribution $\Gamma_{1,e}$ results from the interaction between the magnetic moments of the protons and the conduction electrons, and it follows the Korringa relation [24]

$$T/\Gamma_{1,e} = c_K. \tag{4}$$

Below temperatures of about 200 K the Γ_1 data clearly show Korringa behavior with $c_K = 26.7$ Ks for $LaNi_{5.0}H_{6.0}$ and $c_K = 17.5$ Ks for $LaNi_{4.8}Sn_{0.2}H_{5.8}$ (see dashed lines in Fig. 3). Providing that the dipole–dipole interaction between the hydrogen nuclei and the host nuclei is negligible, the dipolar spin-lattice relaxation rates are given by the relations [10]

$$\Gamma_{1,d} = 3/2\gamma^4\hbar I_H(I_H+1)\Big[J^{(1)}(\omega_0) + J^{(2)}(2\omega_0)\Big], \tag{5}$$

$$\Gamma_{1\rho,d} = 3/8\gamma^4\hbar I_H(I_H+1)\Big[J^{(0)}(2\omega_1) + 10\cdot J^{(1)}(\omega_0) + J^{(2)}(2\omega_0)\Big]. \tag{6}$$

I_H denotes the spin quantum-number of hydrogen and $J^{(q)}(\omega)$ are the spectral density functions, which are obtained by Fourier-transformation of the correlation functions describing the time-dependence of the dipolar interactions. The simplest approximation are correlation functions that decay exponentially with time, as proposed in the BPP-model [9]. The solid lines in Fig. 3 represent fits of Eqs. (3) and (6) to the high-temperature sides of the $\Gamma_{1\rho}$ maxima using the BPP-model and the Korringa

product deduced from the Γ_1 data below 200 K. The obtained activation enthalpies are $H_a = 0.31$ eV for $LaNi_{5.0}H_{6.0}$ and $H_a = 0.24$ eV for $LaNi_{4.8}Sn_{0.2}H_{5.8}$. A similar fit to the $\Gamma_{1\rho}$ data at low temperatures reveals significantly smaller activation enthalpies, indicating a temperature dependence of the activation enthalpies of hydrogen motion in $LaNi_{5.0}H_{6.0}$ and $LaNi_{4.8}Sn_{0.2}H_{5.8}$. Table 1 gives a comparison of the H_a values measured by APFG-NMR with those values that have been deduced from the $\Gamma_{1\rho}$ data in the indicated temperature ranges. A decrease in H_a with decreasing temperature has been reported previously for hydrogen diffusion in $LaNi_5H_x$ [5]. It is interesting to note that the H_a values deduced from the high-temperature sides of the $\Gamma_{1\rho}$ curves agree within the experimental uncertainty with those measured by APFG-NMR. The $\Gamma_{1\rho}$ maximum for $LaNi_{5.0}H_{6.0}$ is observed at about 210 K. With the diffusion parameters given in table 1 follows that $D(210\,\mathrm{K}) = 2.2{\cdot}10^{-14}\ \mathrm{m^2 s^{-1}}$ for $LaNi_{5.0}H_{6.0}$ and that the same diffusion coefficient is expected for $LaNi_{4.8}Sn_{0.2}H_{5.8}$ at about 180 K. The fact that the $\Gamma_{1\rho}$ maximum for $LaNi_{4.8}Sn_{0.2}H_{5.8}$ is, indeed, observed at about 180 K indicates that there is neither a pronounced change in the mechanism of long-range diffusion nor any localized motion between about 180 K and 360 K.

The anomalous temperature behavior of the proton relaxation times found for β-$LaNi_5H_x$ and related systems lead to the proposition that hydrogen motion consists of simultaneous localized hopping and long-range diffusion processes [5]. Recent quasi-elastic and inelastic neutron scattering studies [25, 26] on single-crystal α-$LaNi_5H_x$ stongly support this viewpoint. The neutron scattering data indicated localized motion was confined within hexagons of the 6m hydrogen sites. While differences in occupancy of these between the α and β-phases could influence localized motion, we believe the same basic process is present in both phases as reflected in the proton relaxation times.

sample	source	T-range [K]	H_a [eV]	D_0 [10^{-7} m^2s^{-1}]	D(300 K) [10^{-12} m^2s^{-1}]
$LaNi_5H_{6.0}$	APFG	310 – 365	0.29	3.4	4.6
	$\Gamma_{1\rho}$	210 – 300	0.31		
		160 – 200	0.18		
$LaNi_{4.8}Sn_{0.2}H_{5.8}$	APFG	270 – 350	0.22	0.36	9.2
	$\Gamma_{1\rho}$	180 – 300	0.24		
		120 – 170	0.11		

Table 1: Parameters of the hydrogen diffusion in $LaNi_{5.0}H_{6.0}$ and $LaNi_{4.8}Sn_{0.2}H_{5.8}$

obtained by fitting an Arrhenius expression $D = D_0 \cdot \exp(-H_a/k_B T)$ to the APFG-results. Estimated uncertainties are ± 5 % in the activation enthalpies H_a and ± 20 % in the pre-exponential factors D_0. The diffusivities at 300 K, D(300 K), have been calculated from the fitting parameters. The H_a values deduced from the $\Gamma_{1\rho}$ data in the indicated temperature ranges are included for comparison.

4. Summary

Direct measurements of the hydrogen diffusivity in $LaNi_{5.0}H_{6.0}$ and $LaNi_{4.8}Sn_{0.2}H_{5.8}$ were possible by using alternating pulsed field gradients (APFG). Field gradients up to 25 T/m permitted to extend the temperature range compared to previous APFG-measurements on $LaNi_5H_{6.5}$. The activation energies H_a and prefactors D_0 obtained are H_a = 0.29 eV, $D_0 = 3.4 \cdot 10^{-7}$ $m^2 s^{-1}$ for $LaNi_{5.0}H_{6.0}$ and H_a = 0.22 eV, $D_0 = 3.6 \cdot 10^{-8}$ $m^2 s^{-1}$ for $LaNi_{4.8}Sn_{0.2}H_{5.8}$.

Acknowledgment

We thank Dr. A. Attalla for assistance with the relaxation time measurements on the $LaNi_{4.8}Sn_{0.2}H_{5.8}$ sample. This research was partially supported by the United States Department of Energy under Grant DE-FG03-94ER14493. The Jet Propulsion Laboratory is operated by the California Institute of Technology under contract with the U.S. National Aeronautics and Space Administration. Travel support provided by the North Atlantic Treaty Organization through Grant No. 910179 is gratefully acknowledged.

Figure Captions

Fig. 1

Alternating pulsed field gradient (APFG) sequence. The echo amplitude at $t = 10 \cdot \tau$ is a function of the diffusion coefficient. The deviation of the gradient pulses from a rectangular shape is somewhat exaggerated. The background gradients (G_0) are not shown.

Fig. 2

Diffusion coefficients D of hydrogen in $LaNi_{5.0}H_{6.0}$ and $LaNi_{4.8}Sn_{0.2}H_{5.8}$ measured by APFG-NMR. The solid lines represent fits of Arrhenius terms to the diffusivities. The fit parameters are given in table 1. For comparison, a fit to the diffusivities measured

by Karlicek and Lowe [12] on $LaNi_5H_{6.5}$ is included as a dashed line.

Fig. 3

Proton spin-lattice relaxation rates measured in the laboratory frame (Γ_1) and in the rotating frame ($\Gamma_{1\rho}$). The Γ_1 data are taken at $\omega_0/2\pi = 34.5$ MHz. The $\Gamma_{1\rho}$ measurements were performed at $\omega_0/2\pi = 34.5$ MHz and $\omega_1/2\pi = 31.0$ kHz for $LaNi_{4.8}Sn_{0.2}H_{5.8}$ and at $\omega_0/2\pi = 45.7$ MHz and $\omega_1/2\pi = 31.0$ kHz for $LaNi_{5.0}H_{6.0}$. The dashed lines represent fits of Eq. (4) to the Γ_1 data below 200 K. The corresponding Korringa products are $c_K = 26.7$ Ks for $LaNi_{5.0}H_{6.0}$ and $c_K = 17.5$ Ks for $LaNi_{4.8}Sn_{0.2}H_{5.8}$. The solid lines are fits of Eq. (3) with a BPP-model for $\Gamma_{1\rho,d}$ to the $\Gamma_{1\rho}$ data on the high-temperature sides of the $\Gamma_{1\rho}$ maxima. A fit to the data on the low-temperature side gives significantly smaller activation enthalpies (compare table 1).

References

[1] R.G. Barnes, W.C. Harper, S.O. Nelson, D.K. Thome, and D.R. Torgeson, *J. Less-Common Met.* **49**, 483 (1976).

[2] T.K.. Halstead, *J. Solid State Chem.* **11**, 114 (1974).

[3] T.K.. Halstead, N.A. Abood, and K.H.J. Buschow, *Solid State Commun.* **19**, 425 (1976).

[4] R.F. Karlicek, Jr. and I.J. Lowe, *J. Less-Common Met.* **73**, 219 (1980).

[5] F.E. Spada, H. Oesterreicher, R.C. Bowman, Jr., and M.P. Guse, *Phys. Rev. B* **30**, 4909 (1984).

[6] H. Chang, I.J. Lowe and R.F. Karlicek, in: E.N. Kaufmann and G.K. Shenoy (eds.), *Nuclear and Electron Resonance Spectroscopies Applied to Materials Science*, Elsevier, Amsterdam, p.331 (1981).

[7] R.C. Bowman Jr., D.M. Gruen, and M.H. Mendelsohn, *Solid State Commun.* **32**, 501 (1979).

[8] R.C. Bowman Jr., B.D. Craft, A. Attalla, M.H. Mendelsohn, and D.M. Gruen, *J. Less-Common Met.* **73**, 227 (1980).

[9] N. Bloembergen, E.M. Purcell, and R.M. Pound, *Phys. Rev.* **73**, 679 (1948).

[10] R.M. Cotts, in: G. Alefeld and J. Völkl (eds.), *Hydrogen in Metals I*, Springer, Berlin etc., p.227 (1978).

[11] R.F. Karlicek, Jr. and I.J. Lowe, *J. Magn. Res.* **37**, 75 (1980).

[12] R.F. Karlicek, Jr. and I.J. Lowe, *Solid State Commun.* **31**, 163 (1979).

[13] S. Luo, W. Luo, J. Clewley, T. Flanagan, and L. Wade, *J. Alloys and Compounds* **231**, 467 (1995).

[14] 13. S. Luo, W. Luo, J. Clewley, T. Flanagan, and R. Bowman, *J. Alloys and Compounds* **231**, 473 (1995).

[15] R. C. Bowman, Jr., C. H. Luo, C. C. Ahn, C. K. Witham, and B. Fultz, *J. Alloys and Compounds* **217**, 185 (1995).

[16] B. V. Ratnakumar, C. Witham, R. C. Bowman, Jr., A. Hightower, and B. Fultz, *J. Electrochem. Soc.* **143**, 2578 (1996).

[17] G. Majer, W. Renz, A. Seeger, and R.G. Barnes, *Z. Phys. Chem.*, **181**, 187 (1993).

[18] G. Majer, W. Renz, and R.G. Barnes, *J. Phys.: Condens. Matter*, **6**, 2935 (1994).

[19] U. Kaess, M. Stoll, G. Majer, D.T. Peterson, and R.G. Barnes, *J. Alloys and Compounds* **259**, 74 (1997).

[20] R.G. Barnes, in: H. Wipf (ed.), *Hydrogen in Metals III*, Springer, Berlin etc., p.93 (1997).

[21] D. Richter, R. Hempelmann, and L. Vinhas, *J. Less-Common Met.* **88**, 353 (1982).

[22] H. Züchner, T. Rauf, and R. Hempelmann, *J. Less-Common Met.* **172**, 611 (1991).

[23] N. Mommer, M. Hirscher, and H. Kronmüller, *J. Alloys and Compounds* **253-254**, 390 (1997).

[24] J. Korringa, *Physica* **16**, 601 (1950).

[25] C. Schönfeld, R. Hempelmann, D. Richter, T. Spring, and A. J. Dianoux, *Physica B* **180& 181**, 697 (1992).

[26] C. Schönfeld, R. Hempelmann, D. Richter, T. Spring, A. J. Dianoux, J.J. Rush, T. J. Udovic, and S. M. Bennington, *Phys. Rev. B* **50**, 853 (1994).

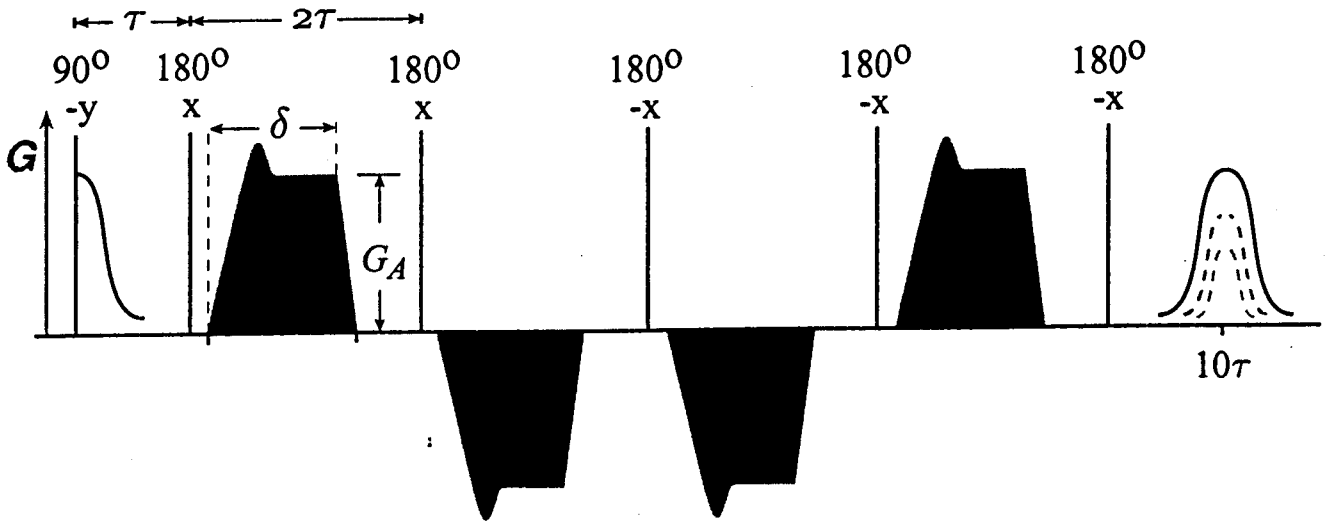

Fig. 1

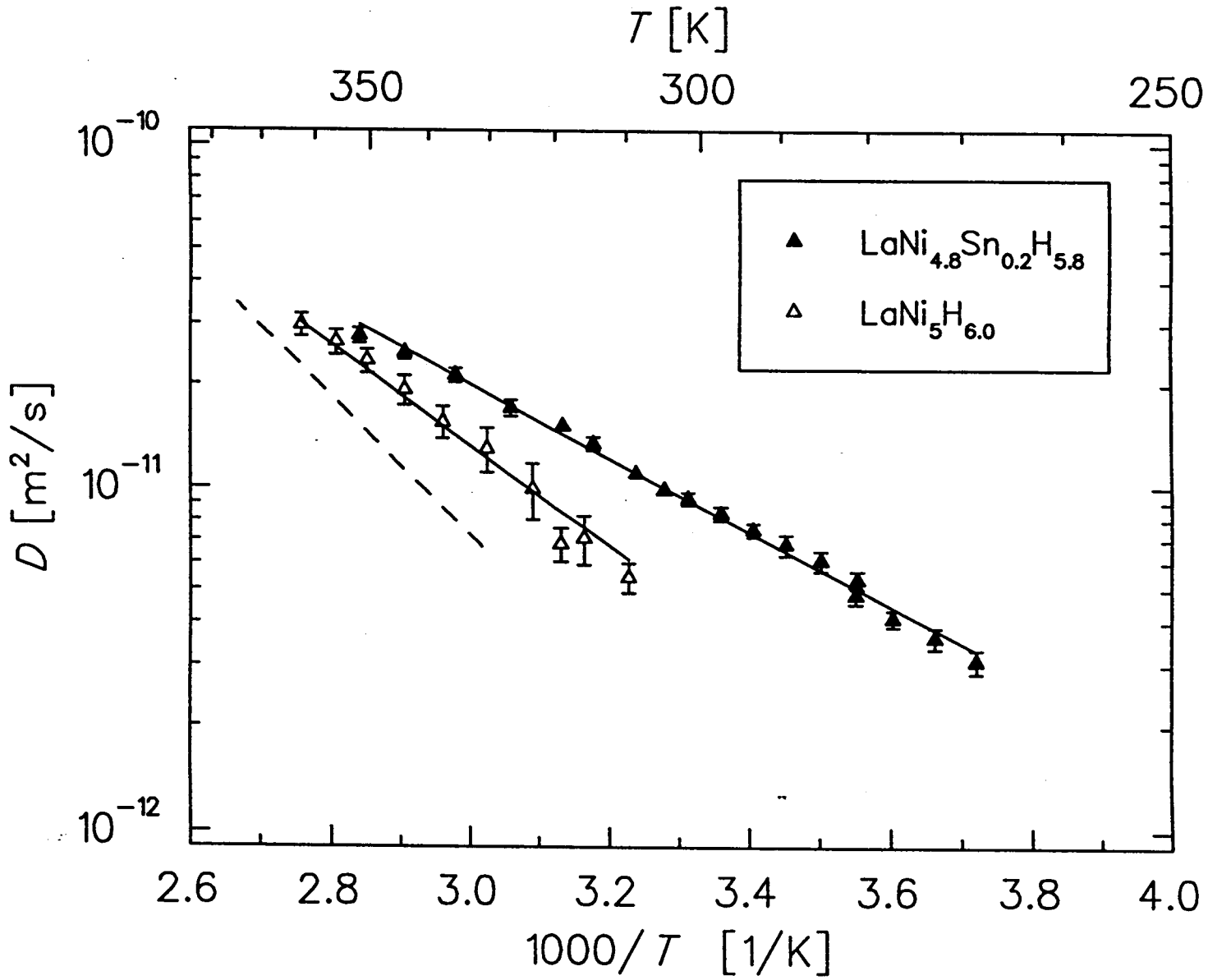
T [K]
350
300
250
10^{-10}
10^{-11}
10^{-12}
D [m²/s]
$LaNi_{4.8}Sn_{0.2}H_{5.8}$
$LaNi_5H_{6.0}$
2.6
2.8
3.0
3.2
3.4
3.6
3.8
4.0
1000/ T [1/K]

Fig. 2

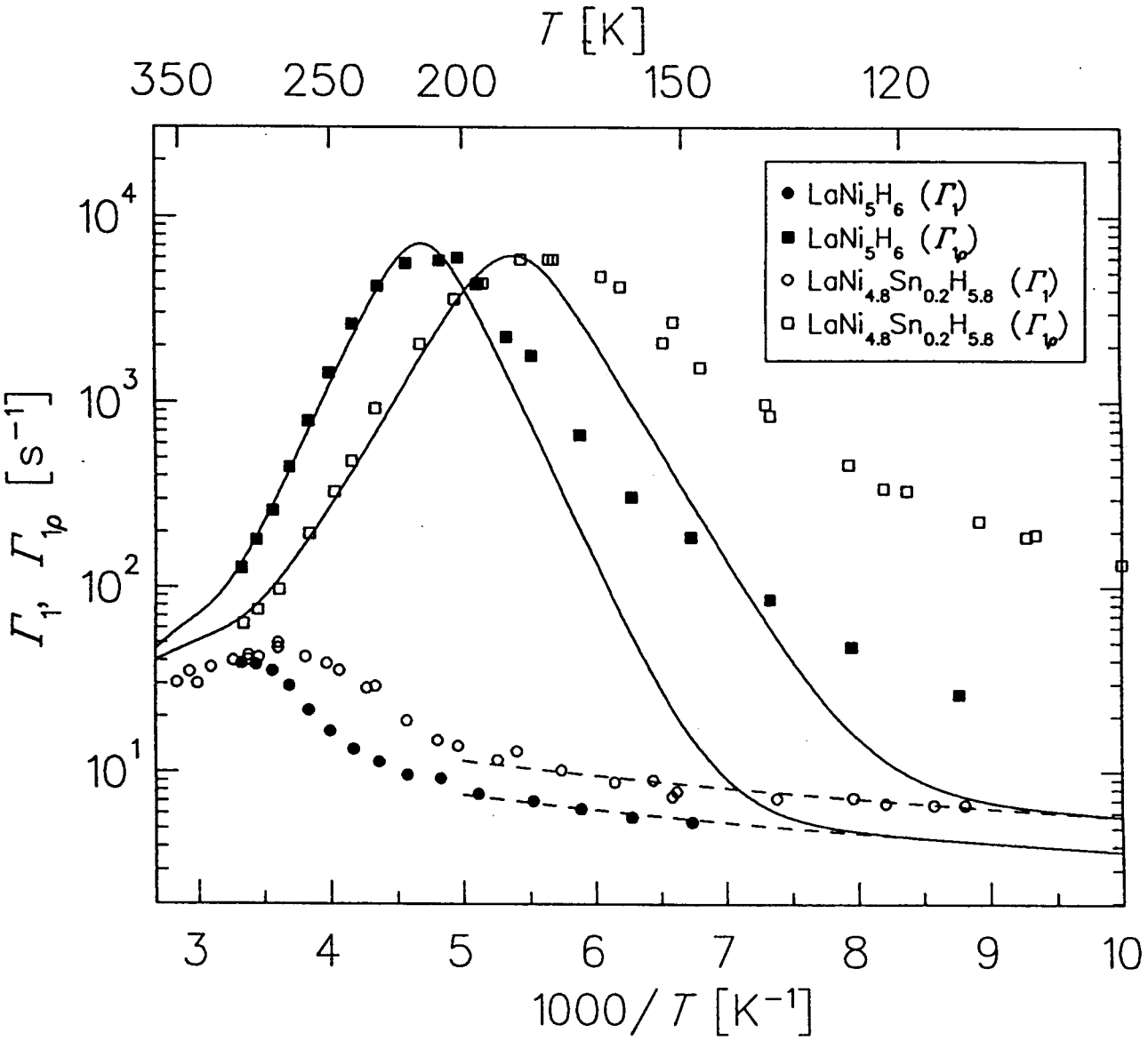
T [K]
350
250
200
150
120
LaNi5H6 (Γ1)
LaNi5H6 (Γ1ρ)
LaNi4.8Sn0.2H5.8 (Γ1)
LaNi4.8Sn0.2H5.8 (Γ1ρ)
Γ1, Γ1ρ [s−1]
10^4
10^3
10^2
10^1
3
4
5
6
7
8
9
10
1000/T [K−1]

Fig. 3